# $\Delta$ mass in quasifree $\Delta$ production from $^{12}$C

Swapan Das
*Nuclear Physics Division, Bhabha Atomic Research Centre, Mumbai-400 085, India*
(Received 9 January 2004; published 15 September 2004)

The quasifree $\Delta^{++}$ production mechanism in charge exchange reactions on the $^{12}$C nucleus has been studied here in the framework of the DWIA. In this study, the $\Delta^{++}$ is assumed to be produced in a one-step process through the elementary $pp \to n\Delta^{++}$ reaction. Since the charge exchange reaction on a nucleus is localized in the low density region, the Lagrangian for describing the $\Delta$ excitation in the nucleus is taken from the study of the free $pp \to n\Delta^{++}$ reaction. The present calculation explores the $\Delta$ mass in the nucleus phenomenologically, so that the calculated results could reproduce both the $\pi^+p$ invariant mass distribution and the ejectile energy distribution spectra.

DOI: 10.1103/PhysRevC.70.034604 PACS number(s): 25.40.Ve, 25.40.Kv, 14.20.Gk

## I. INTRODUCTION

During the last few decades, extensive theoretical and experimental investigations have been reported on the $\Delta(1232)P_{33}$ excitation in the nucleon as well as in the nucleus (see Ref. [1], and references therein). These investigations conclude that this $\Delta$ isobar, like a nucleon, plays an important role as a degree of freedom in the nuclear dynamics at intermediate energies. A prominent signature of the $\Delta$ excitation was seen in inclusive measurements on various nuclear reactions, such as the $(p,n)$ [2] and $(^3\mathrm{He},t)$ [3,4] reactions on the proton as well as on various nuclear targets. In the setup for these measurements, the energy or momentum distribution for the ejectile, e.g., $n$ in $(p,n)$ and $t$ in $(^3\mathrm{He},t)$ reactions, was measured in the forward direction without detecting any other particle emitted in coincidence. The most remarkable aspect seen in these experiments was a large energy shift ($\sim$70 MeV) for the $\Delta$ peak toward the higher ejectile energy in all nuclear targets relative to the hydrogen target [2,3]. However, such a shift was not observed in the $\gamma$-induced [5] and the inclusive $(e,e')$ reactions [6].

To resolve the origin for this $\Delta$-peak shift, some time back exclusive measurements were done on the $(p,n)$ reaction at KEK by Chiba *et al.* [7] and on the $(^3\mathrm{He},t)$ reaction at Saturne by Hennino *et al.* [8,9] on the $^{12}$C target. In this type of experiment, the energy or momentum distribution for the forward going ejectile, i.e., $n$ in the $(p,n)$ and $t$ in the $(^3\mathrm{He},t)$ reactions, was measured in coincidence with various charged particles, like $\pi^+$, $p$, $\pi^+p$, $pp$, etc., emitted within the $4\pi$ direction. In the same setup, the $\pi^+p$ invariant mass distribution, in coincidence with the forward going ejectile was also measured. In these experiments, the outgoing coincident charged particles were detected by a large cylindrical charged particle detector (covering almost the whole solid angle) placed around the target. Analyses of the data for the ejectile energy distribution, obtained from these exclusive measurements, show that both the $pp$ event and the coherent $\pi^+$ production channel contribute to the shift of the inclusive $\Delta$ peak. Among them, the coherent pion production channel contributes dominantly. Contrary to this, the $\pi^+p$ event does not contribute much to the inclusive $\Delta$ peak, but it forms a large portion of the cross sections, specifically, at the higher energy transfer side in the inclusive spectrum. In fact, this is the only channel possible for the hydrogen target. The peak for this channel appearing in the ejectile energy distribution spectrum for the hydrogen target shows an insignificant shift with respect to that for the nuclear targets [8,10]. In contrast to this, the $\pi^+p$ invariant mass distribution spectrum shows a lower $\pi^+p$ mass for the $^{12}$C target nucleus relative to the hydrogen target [7,8].

In this work, the reaction mechanism has been investigated for the $\pi^+p$ event seen (in coincidence with the forward going ejectile) in the exclusive measurements [7,8] done on the charge exchange reactions in the $\Delta^{++}(1232)$ excitation region. According to the present model, the projectile in the charge exchange reactions interacts with a proton bound in the target nucleus. Due to this interaction, the proton in the target gets excited to $\Delta^{++}$, i.e., the $\Delta$ isobar is assumed to be produced in a single step process. Since nucleon-induced nuclear reactions (in the energy region considered here) are localized in the low density region, the $\Delta^{++}$ production in these reactions presumably occurs in this region of the nucleus [11]. Being an unstable particle ($\tau \sim 10^{-23}$ sec), this $\Delta$ isobar decays into $\pi^+$ and $p$ in the continuum. In the exclusive measurements [7,8], these decay products might have been registered by the charged particle detector in coincidence with the forward going ejectile. Therefore, for a charge exchanged exclusive $(a,b)$ reaction, the ingoing coincident $\pi^+p$ emission from a nucleus can be visualized as: $a+A\ (\equiv p+B) \to b+\Delta^{++}+B$; $\Delta^{++} \to \pi^+ + p$. Here, $(a,b)$ represents a charge exchange reaction, such as $(p,n)$, $(^3\mathrm{He},t)$, etc.

Since the $\Delta^{++}$ production in nuclear reactions, as mentioned above, does not take place deep inside the nucleus, the mechanism for it can be thought of as a quasifree process, occurring due to the underlying elementary $pp \to n\Delta^{++}$ reaction. Consequently, the transition interaction for this process has been taken from the study of the free $pp \to n\Delta^{++}$ reaction. For the latter reaction, theoretical investigations by Dmitriev *et al.* [12] and Jain *et al.* [13] show that the use of the one-pion exchange interaction is sufficient to reproduce well the measured spin averaged cross sections over a wide range of energy. The use of the one-pion exchange potential for the $\Delta$

 

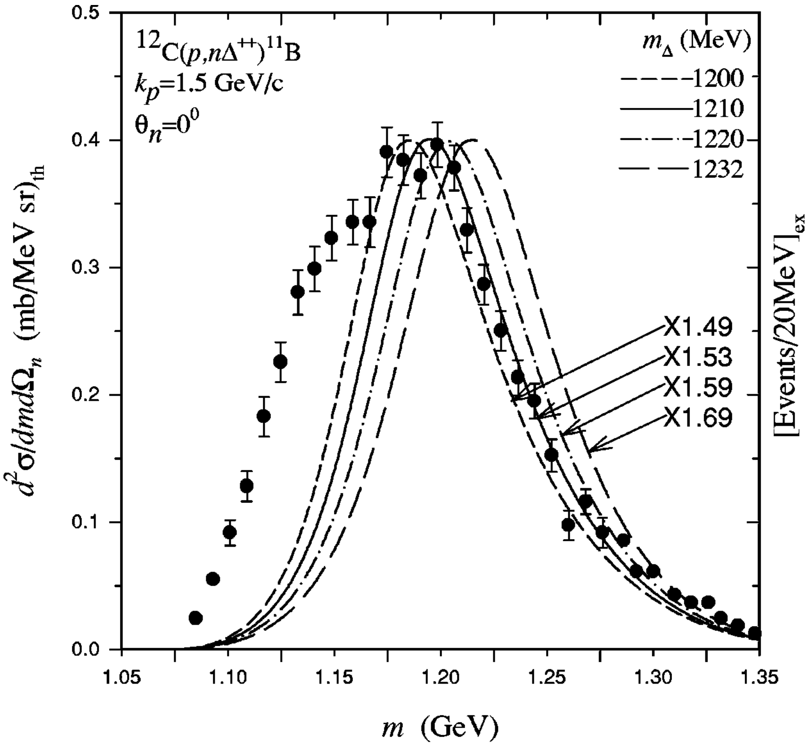


FIG. 1. Calculated $\Delta^{++}$ mass distribution spectra for the $(p,n)$ reaction on the $^{12}$C nucleus are compared with the measured $\pi^+p$ invariant mass distribution spectrum [7] for this reaction. The short dashed, solid, dot dashed, and long dashed lines represent calculated results for $m_\Delta$ in Eq. (15) taken equal to 1200, 1210, 1220, and 1232 MeV respectively.

excitation in nuclear reactions is also quite successful in reproducing the data for the spin averaged cross sections (see Ref. [14], and references therein).

The reaction mechanism for $\Delta^{++}$ production in the $(a,b)$ reaction on the $^{12}$C nucleus has been studied here to analyze the data for the $\pi^+p$ event seen in the exclusive measurements, done at KEK on the $(p,n)$ reaction [7] and at Saturne on the $(^3\mathrm{He},t)$ reaction [8] on the same nucleus. It should be mentioned that several studies [15,16] could successfully reproduce the measured ejectile energy and momentum distribution spectra, but any calculation on the $\pi^+p$ invariant mass distribution spectrum has not been reported yet. Since the $\pi^+p$ emission from the nucleus has been thought of as due to the decay of $\Delta^{++}$ in the continuum, the measured $\pi^+p$ invariant mass distribution spectrum is compared with the calculated mass distribution spectrum for the $\Delta^{++}$ isobar. This comparison (presented in Figs. 1 and 4 below) shows that the $\Delta$ mass taken equal to 1232 MeV (free space value) cannot reproduce the measured $\pi^+p$ invariant mass distribution spectrum. On the other hand, the calculated ejectile energy distribution spectrum for this value of $\Delta$ mass (shown in Figs. 2 and 5 below) reproduces the measured distribution. In this study, it is emphasized that the $\Delta$ mass should change slightly from its free space value, since the $\Delta$ isobar is produced in the low density region of the nucleus. Therefore, the value of the $\Delta$ mass has been explored phenomenologically in this calculation, so that the calculated results can reproduce both the measured $\pi^+p$ invariant mass distribution and the measured ejectile energy distribution spectra obtained from the charge exchange reactions.

In Sec. II, the formalism for quasifree $\Delta$ production in the charge exchange reactions is presented. In Sec. III, the calculated results for the $\Delta$ mass distribution as well as the ejectile energy distribution spectra are shown along with the data.

## II. FORMALISM

In the $(a,b\Delta^{++})$ reaction on a nucleus, the $\Delta^{++}$ is assumed to be produced in a one-step process due to the interaction of the projectile $a$ with a proton bound in the target nucleus. This interaction, as mentioned earlier, can be described by one-pion exchange interaction only. The elementary $\pi NN$ interaction at the projectile-ejectile (i.e., $a$-$b$) vertex, in the pseudovector presentation, can be described by

$$\mathcal{L}_{\pi NN} = \frac{fF(q^2)}{m_\pi}\bar{N}\gamma^\nu\gamma^5\tau N\cdot\partial_\nu\pi, \tag{1}$$

where $f$ (=1.008) is the $\pi NN$ coupling constant. $F(q^2)$ denotes the form factor at the $\pi NN$ vertex. In the monopole form, it is given by $F(q^2)=(\Lambda_\pi^2-m_\pi^2)/(\Lambda_\pi^2-q^2)$, where $q^2$ denotes the four-momentum transfer at the $\pi NN$ vertex. The value for the length parameter $\Lambda_\pi$ is taken equal to 700 MeV/$c$. This value for $\Lambda_\pi$ fits a wide range of data for the free $pp\to n\Delta^{++}$ reaction [13]. Since the $\Delta^{++}$ production in the present reaction is assumed to be a quasifree process, the pion mediated spin-isospin $p\to\Delta^{++}$, according to the pseudovector $\pi N\Delta$ coupling, can be written as

$$\mathcal{L}_{\pi N\Delta} = \frac{f'F'(q^2)}{m_\pi}\bar{\Delta}^\nu\mathbf{T}N\cdot\partial_\nu\pi, \tag{2}$$

with $f'$=2.156 the $\pi N\Delta$ coupling constant. $F'(q^2)$ denotes the form factor at the $\pi N\Delta$ vertex. It is assumed to be identical to $F(q^2)$ appearing in Eq. (1).

The $T$ matrix $T_{fi}$ for the $A(a,b\Delta^{++})B$ reaction, in the distorted wave Born approximation, is given by

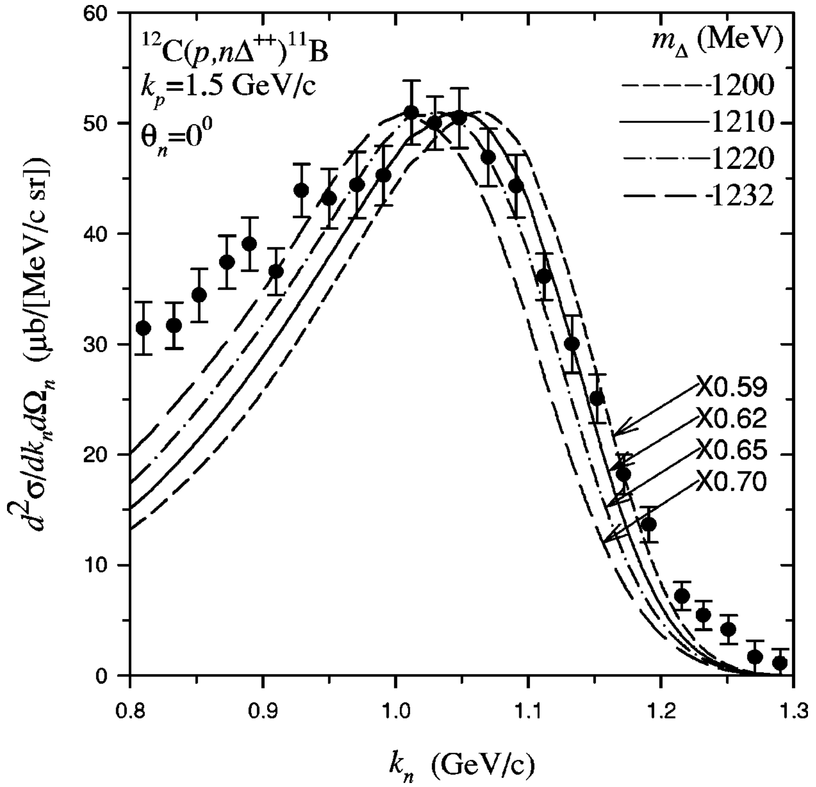


FIG. 2. Calculated forward going neutron momentum distribution spectra for $\Delta^{++}$ production in the $(p,n)$ reaction on the $^{12}$C nucleus are compared with the corresponding measured distribution spectrum for the $\pi^+p$ event seen in coincidence [7]. Various lines are described in Fig. 1.

$$T_{fi} = \langle \chi_b^-, \chi_\Delta^-(b,\Delta,B|V_\pi|A,a)\chi_a^+\rangle, \tag{3}$$

where the $\chi$'s appearing in this equation are the distorted wave functions for particles in the continuum, i.e., the projectile $a$, the ejectile $b$, and the $\Delta$ isobar. In this calculation, these distorted wave functions have been described by the eikonal form. $V_\pi$ denotes the one-pion exchange interaction. In the relativistic presentation, this interaction for the elementary $pp \to n\Delta^{++}$ reaction is given by

$$V_\pi = -\hat{\Gamma}_{\pi NN} G_\pi \hat{\Gamma}_{\pi N\Delta}. \tag{4}$$

In this equation $\hat{\Gamma}_{\pi NN}$ denotes the pion mediated $N \to N$ transition operator at the projectile-ejectile vertex, and $\hat{\Gamma}_{\pi N\Delta}$ describes the pion-induced spin-isospin $p \to \Delta^{++}$ transition operator. They could be described by $\mathcal{L}_{\pi NN}$ in Eq. (1) and $\mathcal{L}_{\pi N\Delta}$ in Eq. (2), respectively, except for the field functions appearing in them. $G_\pi$ represents the pion propagator: $G_\pi(q) = -1/(m_\pi^2 - q^2)$. Here, $m_\pi$ and $q^2$ $(=w^2 - \mathbf{q}^2)$ are the mass and the four-momentum, respectively, for the pion.

Using $V_{\pi^+}$ from Eq. (4), the expression for $T_{fi}$ in Eq. (3) can be factorized as

$$T_{fi} = -\Gamma_{\pi^+ab} G_\pi(q^2)\Gamma(A \to B\Delta^{++}), \tag{5}$$

where $\Gamma_{\pi^+ab}$ represents the matrix element for the $a \to b$ transition. It is given by

$$\Gamma_{\pi^+ab} = (b|\hat{\Gamma}_{\pi NN}|a)\varrho_{ba}(q^2). \tag{6}$$

$\varrho_{ba}(q^2)$ in the above equation denotes the $a \to b$ transition density. If $a$ and $b$ are point particles, $\varrho_{ba}(q^2)$ would be obviously equal to unity. $\Gamma(A \to B\Delta^{++})$, appearing in Eq. (5), denotes the matrix element for the $A \to B\Delta$ transition. The form for it is

$$\Gamma(A \to B\Delta^{++}) = \langle \chi_\Delta^{(-)}, \chi_b^{(-)}(\Delta,B|\hat{\Gamma}_{\pi N\Delta}|A)\chi_a^{(+)}\rangle. \tag{7}$$

After taking an average over the angular momenta in the initial state and a summation over the projection of the angular momenta in the final state, $|T_{fi}|^2$ from the Eq. (5) is given by

$$\langle |T_{fi}|^2\rangle = \langle |\Gamma_{\pi^+ab}|^2\rangle |G_\pi(t)|^2 \langle |\Gamma(A \to B\Delta^{++})|\rangle^2, \tag{8}$$

where $\Gamma_{\pi^+ab}$ and $\Gamma(A \to B\Delta^{++})$ have been described by Eqs. (6) and (7), respectively. For the spin zero target nucleus, i.e., $J=0$, the expression for $\langle |\Gamma(A \to B\Delta^{++})|^2\rangle$ is

$$\langle |\Gamma(A \to B\Delta^{++})|^2\rangle = \langle |\Gamma_{\pi^+p\Delta^{++}}(q^2)|^2\rangle |F_{BA}(\mathbf{Q})|^2. \tag{9}$$

$\langle |\Gamma_{\pi^+p\Delta^{++}}(q^2)|^2\rangle$ represents here the $\pi^+p\Delta^{++}$ vertex factor. It is given by

$$\langle |\Gamma_{\pi^+p\Delta^{++}}(q^2)|^2\rangle = \frac{1}{3}\left|\frac{f'F'(q^2)}{m_\pi}\right|^2 \left[q^2 - \left\{\frac{m^2 - m_N^2 + q^2}{2m}\right\}^2\right]\left[1 + \frac{m^2 + m_N^2 - q^2}{2mm_N}\right]. \tag{10}$$

Here, $m$ and $m_N$ denote the masses for the $\Delta$ isobar and the nucleon, respectively. $F_{BA}(\mathbf{Q})$ appearing in Eq. (9) carries the information about the nuclear structure. It is given by

$$|F_{BA}(\mathbf{Q})|^2 = \sum_{lm} \frac{Z(l)}{2l+1} |G_{nlm}(\mathbf{Q})|^2, \tag{11}$$

where $Z(l)$ is the number of protons in the orbit $l$. $G_{nlm}(\mathbf{Q})$ describes the distorted momentum distribution for a nucleon bound in the nucleus: $G_{nlm}(\mathbf{Q}) = \langle \chi_\Delta^{(-)}, \chi_b^{(-)} | \chi_a^{(+)}, \varphi_{nlm}(\mathbf{r}) \rangle$, with $\mathbf{Q} = \mathbf{k}_a - \mathbf{k}_b - \mathbf{k}_\Delta$. Here, $\varphi_{nlm}(\mathbf{r})$ denotes the spatial part of the wave function for a nucleon bound in the shell "$nlm$" in the target nucleus.

The double differential cross section for the $\Delta^{++}$ mass distribution, in the $(a,b)$ reaction on a nucleus, can be written as

$$\frac{d^2\sigma}{dm\, d\Omega_b} = 2mS(m^2) \int d\Omega_\Delta \int dE_b [KF] \langle |T_{fi}|^2 \rangle. \tag{12}$$

Since the $\Delta^{++}$ can be emitted in any direction, the integration over its emission angle $(\Omega_\Delta)$ has been carried out. The double differential cross section for the ejectile $b$ energy distribution for this reaction is given by

$$\frac{d^2\sigma}{dE_b\, d\Omega_b} \equiv \frac{E_b}{k_b} \frac{d^2\sigma}{dk_b\, d\Omega_b} = \int d\Omega_\Delta \int dm^2\, S(m^2)[KF] \langle |T_{fi}|^2 \rangle. \tag{13}$$

The factor $[KF]$ appearing in this equation represents the kinematical factor for this reaction. The expression for it is

$$[KF] = \frac{m_a m_b m m_B}{(2\pi)^5} \frac{k_b k_\Delta^2}{k_a |k_\Delta (E_i - E_b) - (\mathbf{k}_a - \mathbf{k}_b) \cdot \hat{k}_\Delta E_\Delta|}, \tag{14}$$

where $E_i$ $(=E_a + m_A)$ is the total energy available in the entrance channel in the laboratory system. All other symbols carry their usual meanings.

$S(m^2)$, appearing in Eqs. (12) and (13), denotes the mass distribution function for the $\Delta$ isobar. It has the form

$$S(m^2) = \frac{1}{\pi} \frac{m_\Delta \Gamma_\Delta(m^2)}{[(m^2 - m_\Delta^2)^2 + m_\Delta^2 \Gamma_\Delta^2(m^2)]}, \tag{15}$$

with $m_\Delta$, the mass of $\Delta$ isobar, being equal to 1232 MeV in the free state. $\Gamma_\Delta(m^2)$ represents the width of the $\Delta$ isobar for its mass equal to $m$. It has been provided by analysis of the $\pi^+ p \to \pi^+ p$ reaction data [18], giving

$$\Gamma_\Delta(m^2) = \Gamma_\Delta(m_\Delta^2) \frac{k^3(m^2)}{k^3(m_\Delta^2)} \frac{[k^2(m_\Delta^2) + \gamma_\Delta^2]}{[k^2(m^2) + \gamma_\Delta^2]}, \tag{16}$$

with $\gamma_\Delta = 200$ MeV. $\Gamma_\Delta(m_\Delta^2)$ denotes the width of $\Delta$ in the free state. Its value is taken equal to 120 MeV. $k(m^2)$ is the momentum in the $\pi N$ c.m. system due to the $\Delta$ of mass $m$ decaying at rest.

## III. RESULTS AND DISCUSSION

According to the model presented here, the outgoing coincident $\pi^+ p$ event seen in the exclusive measurements arises due to the decay of the $\Delta^{++}$ in the continuum. The first experiment of this kind, where the $\pi^+ p$ emission was seen in the $(p,n)$ reaction on $^{12}$C target, was performed by Chiba *et al.* at KEK [7]. In the second exclusive measurement, done by Hennino *et al.* at SATURNE [8], the $\pi^+ p$ event was seen in the $(^3\mathrm{He},t)$ reaction on the $^{12}$C nucleus. Since this $\pi^+ p$ event is assumed to be the decay product of the $\Delta^{++}$ isobar, the reaction $^{12}\mathrm{C}(a,b\Delta^{++})^{11}\mathrm{B}$ studied here can be thought to be compatible with the data obtained from the above exclusive measurements. Here, $(a,b)$ symbolically represents a charge exchange reaction, i.e., either $(p,n)$ or $(^3\mathrm{He},t)$. The calculated double differential cross section for the $\Delta^{++}$ mass distribution, as expressed by Eq. (12), is compared with the measured $\pi^+ p$ invariant mass distribution. The calculated double differential cross section for the ejectile energy distribution is described by Eq. (13). Common inputs, used in both $(p,n)$ and $(^3\mathrm{He},t)$ reactions, are the wave function for a nucleon bound in the $^{12}$C nucleus, and the distorted wave function for the $\Delta^{++}$ appearing in the final state.

The ground state of $^{12}$C nucleus has filled $1s_{1/2}$ and $1p_{3/2}$ shells. In this calculation, contributions from both of these shells have been incorporated incoherently. Here, the harmonic oscillator wave function for the bound nucleon is used. The oscillator length parameter is taken equal to 1.66 fm [17], which is consistent with the electron scattering data on $^{12}$C nucleus.

The distorted wave function $\chi_\Delta$ in Eq. (3), due to the elastic scattering of $\Delta$ on the $^{11}$B nucleus, is approximated by the eikonal form. The optical potential $V_{O\Delta}(\mathbf{r})$ required to generate this wave function, following the high energy ansatz, is given by

$$V_{O\Delta}(\mathbf{r}) = (i + \alpha_{\Delta N}) W_{0\Delta} \varrho(\mathbf{r}) / \varrho(0), \tag{17}$$

where $\alpha_{\Delta N}$ denotes the ratio of real to imaginary parts of the $\Delta$ nucleon scattering amplitude, and $W_{0\Delta}$ represents the imaginary part of the $\Delta$ nucleus optical potential. These quantities are described in Ref. [15]. $\varrho(\mathbf{r})/\varrho(0)$ represents the spatial distribution for $V_{O\Delta}(\mathbf{r})$. It is usually to be approximated by the shape for the nuclear density distribution. For $^{11}$B nucleus, the form for $\varrho(\mathbf{r})$ [19] is given by

$$\varrho(\mathbf{r}) = \varrho(0)[1 + a(r/c)^2] e^{-(r/c)^2}. \tag{18}$$

The parameters $a$ and $c$ appearing in this equation, as extracted from the elastic electron scattering data [19], are equal to 0.811 and 1.69 fm, respectively.

### A. $\Delta^{++}$ production in the $(p,n)$ reaction

For the $(p,n)$ reaction, the vertex factor $\langle |\Gamma_{\pi ab}|^2 \rangle$ in Eq. (8) at the $\pi^+ NN$ vertex, due to the pseudovector $\pi NN$ interaction, is given by

$$\langle |\Gamma_{\pi ab}|^2 \rangle \equiv \langle |\Gamma_{\pi^+ pn}(q^2)|^2 \rangle = -2 \left| \frac{fF(q^2)}{m_\pi} \right|^2 q^2, \tag{19}$$

where $q^2$ $[=(E_p - E_n)^2 - (\mathbf{k}_p - \mathbf{k}_n)^2]$ is the four-momentum transfer to the nucleus.

The distorted wave functions appearing in Eq. (3) for the proton and the neutron elastically scattered by the $^{12}$C and $^{11}$B nuclei, respectively, are also approximated by the eikonal form. These wave functions have been generated by the op-

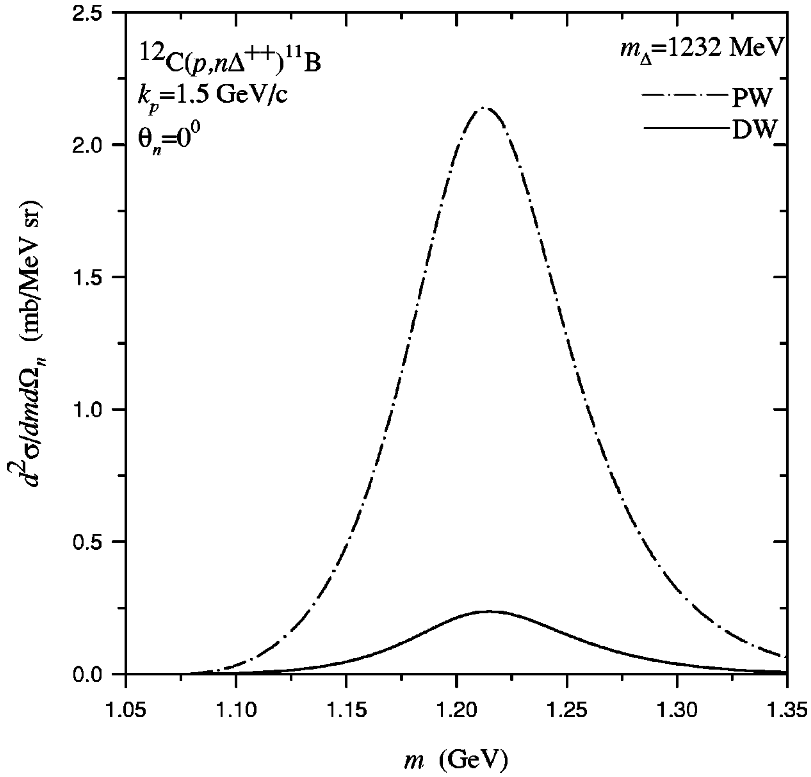


FIG. 3. Calculated $\Delta^{++}$ mass distribution spectra in the $(p,n)$ reaction using plane waves (dot dashed line) and distorted waves (solid line) for $p$, $n$, and $\Delta^{++}$ are presented. In these calculations, $m_\Delta$ in Eq. (15) is taken equal to 1232 MeV.

tical potential $V_{ON}(\mathbf{r})$ which, at intermediate energies, has the form $V_{ON}(\mathbf{r})=(i+\alpha_{NN})W_{0N}\varrho(\mathbf{r})/\varrho(0)$. Here, $N$ represents either a proton or a neutron. The form of $\varrho(\mathbf{r})$ for the $^{12}$C nucleus is also given by Eq. (18), except for the values for $a$ and $c$ taken equal to 1.247 and 1.649 fm, respectively [19]. To evaluate $V_{ON}(\mathbf{r})$, the energy dependent measured values for $\alpha_{NN}$ and $\sigma_t^{NN}$ (required to estimate $W_{0N}$ [14]) are taken from Ref. [20].

The double differential cross sections for the $\Delta^{++}$ mass distribution, $d^2\sigma/dm\,d\Omega_n$ in Eq. (12), and the neutron momentum distribution, $d^2\sigma/dk_n\,d\Omega_n$ in Eq. (13), for the $^{12}$C$(p,n\Delta^{++})^{11}$B reaction have been calculated here. In these calculations, the beam momentum is taken equal to 1.5 GeV/$c$ and the neutron emission angle is taken equal to 0°, since these were the kinematical settings for the exclusive measurement done on the $^{12}$C$(p,n)$ reaction, with the $\pi^+p$ event seen in coincidence, at KEK by Chiba *et al.* [7]. In Fig. 1, the calculated Δ mass distribution spectra for $m_\Delta$, appearing in Eq. (15), taken equal to 1200, 1210, 1220, and 1232 MeV, are presented along with the data for the $\pi^+p$ invariant mass distribution. The calculated spectrum for $m_\Delta$ equal to 1232 MeV, i.e., the mass of Δ in the free state, distinctly fails to reproduce the peak position appearing in the measured spectrum. But the calculated results for $m_\Delta$ equal to 1200 and 1210 MeV are well in accord with the data around the peak and onward. Of course, among them the calculated result for $m_\Delta$ equal to 1200 MeV reproduces the measured peak better. In Fig. 2, the calculated neutron momentum distribution spectra for various values of $m_\Delta$, as mentioned above, are compared with the measured distribution. In this case, the calculated spectrum for the $m_\Delta$ taken equal to 1200 MeV fails to reproduce the measured peak position. Therefore, Figs. 1 and 2 exhibit that the calculated results for $m_\Delta$ taken equal to 1210 MeV reproduce both the measured $\pi^+p$ invariant mass and neutron momentum distribution spectra.

It is noticeable that the present calculations, which consider the Δ excitation in the target nucleus, underestimate cross sections in the region below the peak position. This discrepancy can be accounted for due to the unavoidable drawback arising in the $(p,n)$ reaction to probe the Δ excitation in the nucleus. The dynamics of the neutron arising due to the decay of the Δ isobar as well as the quasifree knockout from the target nucleus were also measured in this reaction. Cross sections due to these neutrons, for an obvious reason, contribute in the region below the peak position. This drawback, as shown later, cannot arise in the $(^3\text{He},t)$ reaction, since the probability of the excited $^3$He decaying to triton and the quasifree knockout of the triton from the target nucleus are expected to be very small [21,22].

As mentioned in Ref. [7], the geometry of the charged particle detector used for the exclusive measurement on the $(p,n)$ reaction is such that it cannot register all $\pi^+p$ events in coincidence. For the hydrogen target, where only the $\pi^+p$ event is possible, this setup showed a detecting efficiency of about 65%. A little change in this efficiency may be expected for the $^{12}$C target, since many other channels are also possible for this nucleus. Therefore, it is remarkable that the calculated neutron momentum distribution, as shown in Fig. 2, reproduces the data very well.

It is always advisable to investigate the initial and final state interactions in nuclear reactions. Therefore, the calculated Δ mass distribution spectrum, using the plane waves for $p$, $n$, and $\Delta^{++}$, has been plotted in Fig. 3 along with the calculated distorted wave results. Both of these spectra are generated for the input Δ mass taken equal to 1232 MeV (free space value) in Eq. (15). This figure exhibits that the

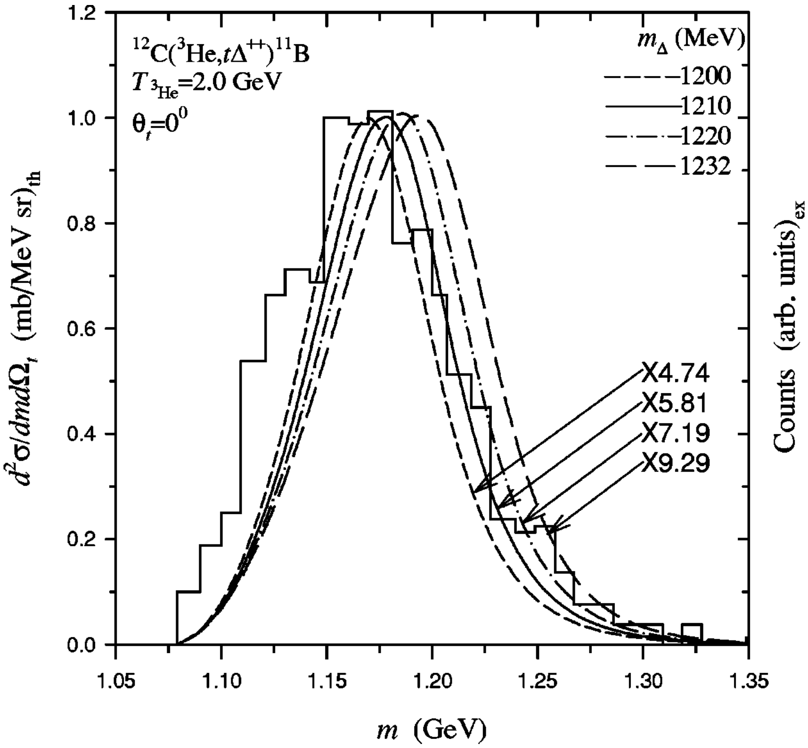


FIG. 4. Calculated $\Delta^{++}$ mass distribution spectra for the ($^3$He,$t$) reaction on the $^{12}$C nucleus are compared with the measured $\pi^+p$ invariant mass distribution spectrum [8] for this reaction. Various lines are described in Fig. 1.

effect of distortions, due to the elastic scattering of the continuum particles, on the cross section is purely absorptive. It reduces the plane wave result by a factor of about 9 at the peak, retaining the shape of the $\Delta$ mass distribution spectrum unaltered. Therefore, the small reduction in the $\Delta$ mass ($m_\Delta$=1210 MeV), which brings the calculated results well into accord with the measured spectra, may be thought to be due to the nuclear medium effect. Indeed, this mass reduction cannot be drastic, since the $\Delta$ is produced, as mentioned earlier, in the low density region of the nucleus.

### B. $\Delta^{++}$ production in ($^3$He,$t$) reaction

There are two major ways where the ($^3$He,$t$) reaction differs from the $(p,n)$ reaction. These differences are the helium-3 to triton transition density (appearing in the $\pi^+\,{}^3$He$t$ vertex) and the distortion functions for helium-3 and triton nuclei. For the pseudovector $\pi NN$ coupling, the $\langle|\Gamma_{\pi ab}|^2\rangle$ in Eq. (8) at the $\pi^+\,{}^3$He$t$ vertex is given by

$$\langle|\Gamma_{\pi ab}|^2\rangle \equiv \langle|\Gamma_{\pi^+ht}(q^2)|^2\rangle = -\frac{2}{9}\left|\frac{fF(q^2)}{m_\pi}\varrho_{ht}(q^2)\right|^2 q^2, \tag{20}$$

with $q^2=(E_h-E_t)^2-(\mathbf{k}_h-\mathbf{k}_t)^2$. The symbol "$h$" appearing here represents the $^3$He nucleus only. $\varrho_{ht}(q^2)$ denotes the helium-3$\rightarrow$ triton transition density. This transition density, as required for the high momentum transfer region, is approximated by the magnetic form factor of the $^3$He nucleus: $\varrho_{ht}(q^2)=3[\exp(-a^2q^2)-b^2q^2\exp(-c^2q^2)]$, with $a$=0.654 fm, $b$=0.456 fm, and $c$=0.821 fm. This form factor has been extracted up to $q^2$=16 fm$^{-2}$ by McCarthy *et al.* [23] from the electron scattering data between 170 and 750 MeV on the $^3$He nucleus.

Since the optical potential for the mass-3 nucleus is a poorly known quantity, the distortion functions for $h$ (i.e., $^3$He) and $t$ nuclei can be estimated, in a better way, from their measured phase shift functions. In the eikonal model prescription, these distortion functions can be approximated in terms of the phase shift function $\delta(b)$: $D^{(-)*}_{\mathbf{k}_t}D^{(+)}_{\mathbf{k}_h} \approx \exp[i2\delta(b)]$. This approximation was successfully used earlier by Johnson and Bethe [24] to describe the strong absorption for the pion-induced reaction around (3:3) resonance, and also by Jain and Sarma [25] to account for the distortion for the $(\alpha,2\alpha)$ reaction. For the present calculation at 2 GeV beam energy, $\delta(b)$ is required in the energy region between 1 and 2 GeV. However, in this energy range information about $\delta(b)$ is available in the literature for $\alpha$ scattering at 1.37 GeV on calcium isotopes [26]. Here, $\exp[i2\delta(b)]$, which describes the $\alpha$ elastic scattering data very well, is found to be a purely absorptive quantity. It has the form $\exp[i2\delta(b)]\approx 1/[1+e^{-(b-R)/c}]$, with $c$=0.68 fm and $R=r_0A^{1/3}$ fm ($r_0$=1.45 fm). In the absence of any other available information, this form is usually taken to describe the distortion due to the elastic scattering of $^3$He and $t$ by the nucleus [14,27], except that the value for $r_0$ is reduced to 1.2 fm.

The spectra for the $\Delta^{++}$ mass distribution, $d^2\sigma/dm\,d\Omega_t$ in Eq. (12), and the triton energy distribution, $d^2\sigma/dE_t\,d\Omega_t$ in Eq. (13), have been calculated here for the ($^3$He,$t\Delta^{++}$) reaction on the $^{12}$C nucleus. In the experiment done at Saturne [8], the beam energy was taken equal to 2 GeV and the triton energy was measured at the forward angle. Therefore, the present calculations have been done for such kinematics. As it is done for the $(p,n)$ reaction, the $\Delta^{++}$ mass distribution and the triton energy distribution spectra have been calculated for $m_\Delta$ in Eq. (15) taken equal to 1200, 1210, 1220, and

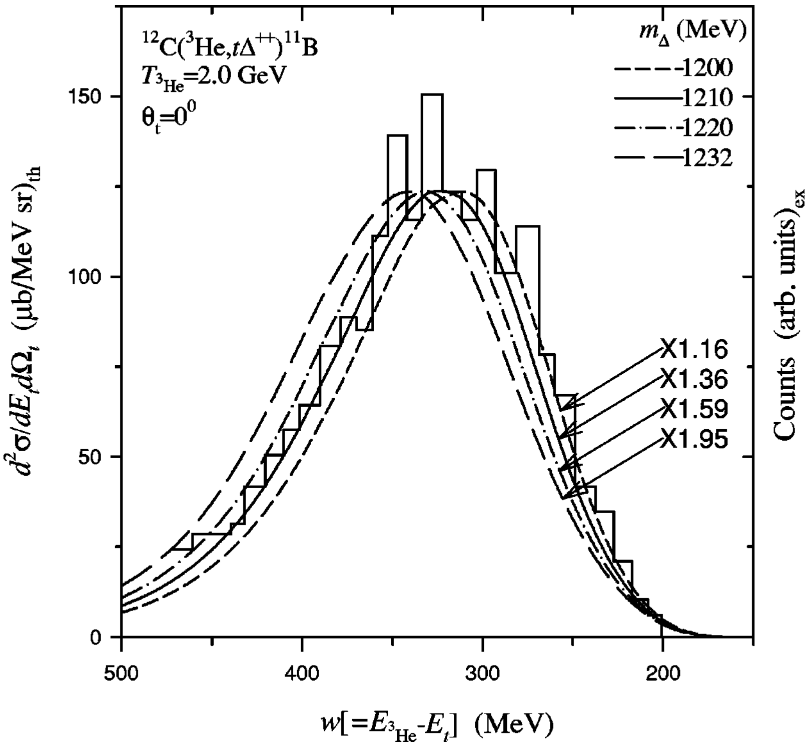


FIG. 5. Calculated energy transfer (from the $^3$He-$t$ vertex) distribution spectra for the $\Delta^{++}$ production in the ($^3$He,$t$) reaction on the $^{12}$C nucleus are compared with the corresponding measured distribution spectrum for the $\pi^+p$ event seen in coincidence [8]. Various lines are described in Fig. 1.

1232 MeV. The calculated Δ mass distribution spectra are compared with the data for the $\pi^+p$ invariant mass distribution in Fig. 4, and the calculated forward going triton energy distribution spectra are shown along with the measured spectrum in Fig. 5. These figures exhibit observations analogous to those for the $(p,n)$ reaction presented earlier. The calculated cross sections for $m_\Delta$ taken equal to 1210 MeV reproduce both the measured $\pi^+p$ invariant mass and triton energy distribution spectra. In this reaction also, the effect of distortions (not shown) due to the in-continuum particles is found purely absorptive. This is quite consistent with the study, as mentioned earlier, on the $(p,n)$ reaction.

## IV. CONCLUSIONS

In the present work, the mechanism for the $\Delta^{++}$ production in $(p,n)$ and ($^3$He,$t$) reactions on the $^{12}$C nucleus has been studied. The $\pi^+p$ event seen in the exclusive measurements done on the above reactions can be accounted for mainly by the direct decay of $\Delta^{++}$ in the continuum. This Δ isobar is produced in a one-step process due to the interaction of the elastically scattered projectile with a proton bound in the target nucleus. The overall distortion due to the elastic scattering of particles appearing in the continuum is purely absorptive. The $\Delta^{++}$ excitation, in the reactions presented here, can be described by the pseudovector one-pion exchange Lagrangian, which reproduces well the wide range of measured cross sections for the free $pp\to n\Delta^{++}$ reaction. The calculated results for the Δ mass $m_\Delta$ phenomenologically reduced to 1210 MeV (from its free space value, i.e., 1232 MeV) are found to reproduce very well both the measured $\pi^+p$ invariant mass distribution and the ejectile energy distribution spectra.

## ACKNOWLEDGMENTS

I am grateful to Dr. S. Kailas for his encouragement and support for this work. I thank P. Roychowdhury for his kind help in preparing this manuscript. I also thank M. J. Consara, E. T. Mirgule, R. G. Thomas, and P. K. Sahu for providing computation facilities.

[1] G. E. Brown and W. Weise, Phys. Rep., Phys. Lett. **22**, 279 (1975); E. Oset, H. Toki, and W. Weise, *ibid.* **83**, 281 (1982); M. Rho, Annu. Rev. Nucl. Part. Sci. **34**, 531 (1984); T. O. Ericson and W. Weise, *Pions in Nuclei* (Clarendon Press, Oxford, 1988); C. Gaarde, Annu. Rev. Nucl. Part. Sci. **41**, 187 (1991); B. K. Jain and A. B. Santra, Phys. Rep. **230**, 1 (1993).
[2] C. W. Bjork *et al.*, Phys. Lett. **63B**, 31 (1976); G. Glass *et al.*, Phys. Rev. D **15**, 36 (1977); D. A. Lind, Can. J. Phys. **65**, 637 (1987); C. G. Cassapakis *et al.*, Phys. Lett. **63B**, 35 (1976); B. E. Bonner *et al.*, Phys. Rev. C **18**, 1418 (1978).
[3] D. Contardo *et al.*, Phys. Lett. **168B**, 331 (1986).
[4] C. Ellegaard *et al.*, Phys. Rev. Lett. **50**, 1745 (1983); Phys. Lett. **154B**, 110 (1985); Can. J. Phys. **65**, 600 (1987); V. G. Ableev *et al.*, JETP Lett. **40**, 763 (1984); D. Bachelier *et al.*, Phys. Lett. B **172**, 23 (1986); I. Bergqvist *et al.*, Nucl. Phys. **A469**, 648 (1987); M. Roy-Stephan, *ibid.* **A488**, 187c (1988).
[5] T. A. Armstrong *et al.*, Phys. Lett. **34B**, 535 (1971); Nucl. Phys. **B41**, 445 (1972); J. H. Koch, E. J. Moniz, and N. Oht-

suka, Ann. Phys. (N.Y.) **154**, 99 (1984); J. Ahrens *et al.*, Phys. Lett. **146B**, 303 (1984); Nucl. Phys. **A466**, 229c (1985); Th. Frommhold *et al.*, Phys. Lett. B **295**, 28 (1992); N. Bianchi *et al.*, *ibid.* **299**, 219 (1993); **309**, 5 (1993); **325**, 333 (1994); M. Anghinolfi *et al.*, Phys. Rev. C **47**, R922 (1993).

[6] J .S. O'Connell *et al.*, Phys. Rev. Lett. **53**, 1627 (1984); Phys. Rev. C **35**, 1063 (1987); R. M. Sealock *et al.*, Phys. Rev. Lett. **62**, 1350 (1989).

[7] J. Chiba *et al.*, Phys. Rev. Lett. **67**, 1982 (1991).

[8] T. Hennino *et al.*, Phys. Lett. B **283**, 42 (1992).

[9] T. Hennino *et al.*, Phys. Lett. B **303**, 236 (1993).

[10] P. Radvanyi *et al.*, in *Hadrons in Nuclear Matter*, edited by H. Feldmeier and W. Nörenberg (GSI, Darmstadt, 1995), p. 44.

[11] B. K. Jain, J. T. Londergan, and G. E. Walkar, Phys. Rev. C **37**, 1564 (1988).

[12] V. Dmitriev, O. Sushkov, and C. Gaarde, Nucl. Phys. **A459**, 503 (1986).

[13] B. K. Jain and A. B. Santra, Int. J. Mod. Phys. E **1**, 201 (1992).

[14] Swapan Das, Phys. Rev. C **66**, 014604 (2002).

[15] B. K. Jain and Swapan Das, Phys. Rev. C **50**, 370 (1994).

[16] B. Körfgen, P. Oltmanns, F. Osterfeld, and T. Udagawa, Phys. Rev. C **55**, 1819 (1997).

[17] U. Meyer-Berkhout *et al.*, Ann. Phys. (N.Y.) **8**, 119 (1959).

[18] V. Flamino, W. G. Moorhead, D. R. O. Morrison, and N. Rivoire, Report No. CERN-HERA 83-01, 1983 (unpublished).

[19] H. De. Vries and C. W. De Jager, At. Data Nucl. Data Tables **14**, 480 (1974).

[20] D. V. Bugg *et al.*, Phys. Rev. **146**, 980 (1966); S. Barshay *et al.*, Phys. Rev. C **11**, 360 (1975); W. Grein, Nucl. Phys. **B131**, 255 (1977); C. Lechanoine-Leluc *et al.*, Rev. Mod. Phys. **65**, 47 (1993); Particle Data Group, R. M. Barnett *et al.*, Phys. Rev. D **54**, 1 (1996).

[21] R. G. Jeppesen, Ph.D. thesis, University of Colorado, 1986.

[22] T. Udagawa, P. Oltmanns, F. Osterfeld, and S. W. Hong, Phys. Rev. C **49**, 3162 (1994).

[23] J. S. McCarthy, I. Sick, and R. R. Whitney, Phys. Rev. C **15**, 1396 (1977).

[24] M. B. Johnson and H. Bethe, Comments Nucl. Part. Phys. **8**, 75 (1978).

[25] B. K. Jain and N. R. Sharma, Nucl. Phys. **A388**, 243 (1982).

[26] D. C. Choudhury, Phys. Rev. C **22**, 1848 (1980).

[27] B. K. Jain, Phys. Rev. C **32**, 1253 (1985); N. G. Kelkar and B. K. Jain, Int. J. Mod. Phys. E **4**, 181 (1995).